Available online at www.sciencedirect.com
ScienceDirect
Journal of Power Sources 174 (2007) 199–205
JOURNAL OF POWER SOURCES
www.elsevier.com/locate/jpowsour

Carbon-coated stainless steel as PEFC bipolar plate material

Tomokazu Fukutsuka [a,*], Takayuki Yamaguchi [a], Shin-Ichi Miyano [a], Yoshiaki Matsuo [a], Yosohiro Sugie [a], Zempachi Ogumi [b]

[a] *Graduate School of Engineering, University of Hyogo, 2167 Shosha, Himeji, Hyogo 671-2280, Japan*
[b] *Graduate School of Engineering, Kyoto University, Nishikyo-ku, Kyoto 615-8510, Japan*

Received 31 July 2007; received in revised form 30 August 2007; accepted 31 August 2007
Available online 5 September 2007

Abstract

Stainless steel is quite attractive as bipolar plate material for polymer electrolyte fuel cells (PEFCs). Passive film on stainless steel protects the bulk of it from corrosion. However, passive film is composed of mixed metal oxides and causes a decrease in the interfacial contact resistance (ICR) between the bipolar plate and gas diffusion layer. Low ICR and high corrosion resistance are both required. In order to impart low ICR to stainless steel (SUS304), carbon-coating was prepared by using plasma-assisted chemical vapor deposition. Carbon-coated SUS304 was characterized by Raman spectroscopy and atomic force microscopy. Anodic polarization behavior under PEFC operating conditions (H_2SO_4 solution bubbled with H_2 (anode)/O_2 (cathode) containing 2 ppm HF at 80 °C) was examined. Based on the results of the ICR evaluated before and after anodic polarization, the potential for using carbon-coated SUS304 as bipolar plate material for PEFC was discussed.

Keywords: PEFC; Bipolar plate; Carbon-coating; Stainless steel; Corrosion

1. Introduction

Fuel cells are very attractive power sources due to their high efficiency and zero-emission capability. Among them, polymer electrolyte fuel cells (PEFCs) have been studied as the power sources of fuel cell vehicles (FCV), portable electronic devices, etc. Commercial application of PEFC requires high durability to achieve long cycle life. The reduction of cost, mass, and volume is necessary. To obtain sufficient battery voltage for FCV use, a stack of single cells using bipolar plates is inevitable because of the low voltage of a single cell. Bipolar plates are multi-functional components. They act as current collectors of cells and separators of the reactive gases between the anode side (hydrogen gas) and cathode side (oxygen gas). Bipolar plates account for the large percent of mass and volume in a PEFC stack [1,2]. Hence, improvement of bipolar plates is essential to the commercial use of FCV.

The requirements for bipolar plates are high electric conductivity, high corrosion resistance, high mechanical strength, high gas impermeability, light material, and low-cost material. So far, various carbonaceous materials have been used as bipolar plates. In order to reduce the size of a PEFC stack or increase the number of single cells in a stack, the use of thin bipolar plates are essential. However, thin carbon-based bipolar plates cannot be used due to their low toughness and gas permeability. On the other hand, metallic materials are very attractive due to their high mechanical strength, leading to thin bipolar plates. Moreover, high electric conductivity in bulk, high mechanical strength, high gas impermeability, lightness, and low-cost are attractive. There is a fatal flaw in metal bipolar plates, since most metals easily corrode under PEFC operating conditions. Dissolution of the metal cation by corrosion impairs the performance of PEFC, such as degradation of the polymer electrolyte membrane [3]. Although novel metals, such as platinum and gold, are generally corrosion-free, they are very expensive. Stainless steel and titanium show high corrosion resistance because of their excellent passive film mainly composed of metal oxide. Although these highly corrosion-resistant metals are desirable, passive films decrease the surface electric conductivity [4,5]. Moreover, these passive films grow gradually under PEFC operation conditions, leading to a decrease in electric conductivity. Since bipolar plates serve as current collectors, high electric

* Corresponding author. Tel.: +81 79 267 4948; fax: +81 79 267 4948.
E-mail address: fuku@eng.u-hyogo.ac.jp (T. Fukutsuka).

0378-7753/$ – see front matter © 2007 Elsevier B.V. All rights reserved.
doi:10.1016/j.jpowsour.2007.08.096

conductivity is essential. Therefore, most metallic materials, without any pretreatment such as surface coating, cannot satisfy both the high corrosion resistance and high electric conductivity requirements.

So far, gold-coating on the surface of stainless steel, aluminum, and titanium has been extensively studied [4,5]. Gold-coating is very expensive and a rather thick film is needed in order to provide sufficient corrosion resistance, so, gold-coating is not suitable for industrial use. We therefore focused on carbon-coating. When a carbon layer acts as a barrier layer that cloaks the active surface area of metals and gives high electric conductivity, various metals can be used as the base materials for bipolar plates. Coating with electric conductive carbon (sp^2-type carbon) on metal has not been thought to be easy, since sp^2-type carbonaceous thin film is porous, which cannot serve as a barrier layer. We recently prepared carbon-coated Fe-based material as a bipolar plate by plasma-assisted chemical vapor deposition (plasma CVD) [6]. In that study, carbon steel (S25C) covered with Ni from electroless plating (Ni-S25C) was used. The resulting carbon-coated Ni-S25C showed quite high electric conductivity. This result showed that no metal oxide between the carbon layer and the metal was formed in the coating process. The corrosion resistance of the resulting carbon-coated Ni-S25C was improved compared with uncoated Ni-S25C. Based on these results, it is considered that carbon-coating by plasma-assisted CVD might be one of the candidate techniques for the practical use of metal bipolar plates. However, this corrosion resistance depended on the electroless Ni plating layer. This result also suggested that optimization of an electroless Ni plating layer is an important factor to achieve adequate properties for a bipolar plate. Hence, using an optimized electroless Ni plating layer might be not suitable for industrial use due to its high cost. But, stainless steel is attractive material due to its high productivity from the perspective of industrial use [7–17].

As mentioned above, passive film on stainless steel protects the bulk of it from corrosion, but it affects the interfacial contact resistance. If a dense carbon layer is coated on the surface of stainless steel whose passive film has been completely eliminated, the interfacial contact resistance will be sufficiently reduced. Moreover, when this carbon layer is locally damaged physically or chemically, passive film on the stainless steel will be rapidly formed and the influence of this locally formed passive film on the interfacial contact resistance may be negligible. Hence, using stainless steel as the base metal in our carbon-coating technique is very interesting. In this paper, the preparation of carbon-coated stainless steel by plasma-assisted CVD and its corrosion properties as bipolar plates for PEFCs were reported.

2. Experimental

2.1. Carbon-coating

Carbon-coating on substrates was carried out by using plasma-assisted CVD from acetylene and argon. The detailed procedure is described in our previous papers [6,18,19]. Briefly, the substrate material is stainless steel (SUS304 containing Si (0.45%), P (0.04%), Cu (0.20%), Cr (18.33%), Ni (8.25%), and Fe (the balance). The substrate was 0.1 mm in thickness and 15 mm square. Before carbon-coating, SUS304 was polished with waterproof abrasive paper (#2000). Noted that only one side of SUS304 was coated with the carbon layer in this study. An unpolished SUS304 was used as a comparison. The substrates were placed on a ground electrode whose temperature was kept at 1053 K and the applied rf power was set at 90 W. The coating time was set at 5 h and the samples were cooled down to 373 K gradually within about 1.5 h. The thickness of the carbon-coating was less than 1 μm.

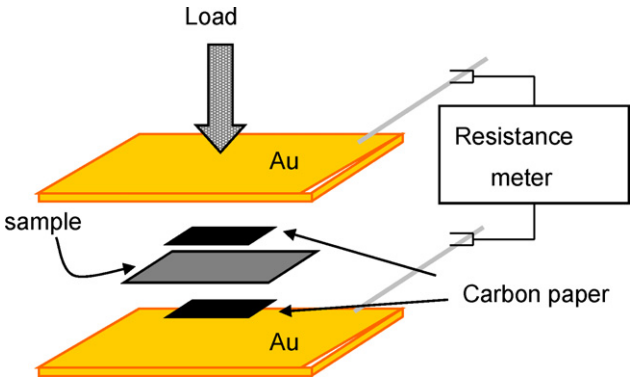

Fig. 1. Schematic illustration of ICR measurement equipment.

2.2. Structural characterization

In order to characterize the carbon-coating on the substrates, Raman measurement (Jobin-Yvon T-64000) and atomic force microscope (AFM) observation (Digital Instruments CP-II) were carried out. The interfacial contact resistance (ICR) of the obtained carbon-coated metal was evaluated by a method similar to that reported by Wang et al. [8]. A schematic illustration of the ICR measurement is shown in Fig. 1. In this measurement, two carbon papers (CP: TORAY TGP-H-120, 1 cm^2) were placed between the sample and two Au plates. The resistance was measured by using a 4-probe resistance meter (TSURUGA model 3569). A compaction force (100 N cm^{-2}) was applied by using IMADA Z2-500N (a digital force gauge) and IMADA HV-500NII (a manual hand wheel operation stand). The measured resistance is expressed as follows:

$$R_{\text{total}} = 2R(\text{Au} + \text{lead}) + 2r(\text{Au/CP}) + 2R(\text{CP}) + r(\text{CP/sample/CP}) + R(\text{sample}), \quad (1)$$

where $R(x)$ is the bulk resistance and $r(x)$ is the interfacial resistance. To calculate the ICR (r(CP/sample/CP)), the R_{base} is given as follows:

$$R_{\text{base}} = 2R(\text{Au} + \text{lead}) + 2r(\text{Au/CP}) + R(\text{CP}). \quad (2)$$

From Eqs. (1) and (2), ICR is calculated as follows:

$$\text{ICR} = R_{\text{total}} - R_{\text{base}} - R(\text{CP}) - R(\text{sample}). \quad (3)$$

Under the assumption that R(sample) is much smaller than other resistances, ICR is calculated from Eq. (3) as follows:

$$\mathrm{ICR} = R_{\mathrm{total}} - R_{\mathrm{base}} - R(\mathrm{CP}). \quad (4)$$

Since R(CP) is obtained from the specification from the supplier, the ICR can be obtained from Eq. (4). Since the apparent surface area of the carbon paper is 1 cm^2 and the current passes vertically, the value of the measured resistance equals the resistivity.

2.3. Electrochemical measurement

All electrochemical measurements were conducted by HSV-100F (HOKUTO-DENKO) using a three-electrode cell. The samples were used as working electrodes. A platinum wire was used as a counter electrode and an Hg/Hg_2SO_4 electrode was used as a reference electrode. Unless otherwise stated, the potential is referenced against Hg/Hg_2SO_4. In order to simulate the electrolyte condition for a bipolar plate under PEFC operating conditions, previous literature was referenced [20]. We selected a 0.5 mol dm^{-3} H_2SO_4 solution (pH 1) as the base electrolyte. The concentrations of fluoride ions (as HF) were 0 or 2 ppm. Prior to measurement, the H_2SO_4 solution was bubbled with N_2, O_2 (cathode environment), or H_2 (anode environment). During measurement, air (cathode environment) or H_2 (anode environment) passed through the gas phase in the cell. Electrochemical experiments were conducted at room temperature or 80 °C. To clarify the dynamic polarization behavior, linear sweep voltammetry was conducted. The electrode potential was swept from −1 V (−0.626 V vs. SCE) to 0.6 V (0.974 V vs. SCE) at a scan rate of 1 mV s^{-1}. Since the electrolyte conditions corresponded to the condition under direct contact with membrane electrode assembly (MEA), it is considered that the electrochemical measurements in this paper were done under accelerated fuel cell conditions.

3. Results and discussion

3.1. Structure and surface morphology of carbon-coating

The Raman spectrum of carbon-coated SUS304 is shown in Fig. 2. The resultant Raman spectrum showed features of sp^2-type carbonaceous materials. In the Raman spectrum, mainly three peaks around 1360 cm^{-1}, 1580 cm^{-1}, and 1620 cm^{-1} were observed. The peak around 1580 cm^{-1} is related to the crystallinity of carbonaceous materials, and is assigned to the Raman active E_{2g} mode frequency (G band) [21]. The peak around 1360 cm^{-1} is ascribed to the Raman inactive A_{1g} mode frequency [21]. The peaks around 1360 cm^{-1} and 1620 cm^{-1} appear in the case of finite crystal size and imperfection of carbonaceous materials and the former is called as D band and the latter is as D′ band. When we focus on the peaks around 1360 cm^{-1}, their intensities are higher than those of the peaks around 1580 cm^{-1}. This characteristic indicates that the size of graphitic crystallite would be small and the number of edge planes would be large. The surface morphology of the carbon-coating on SUS304 was observed by AFM. Fig. 3 shows the

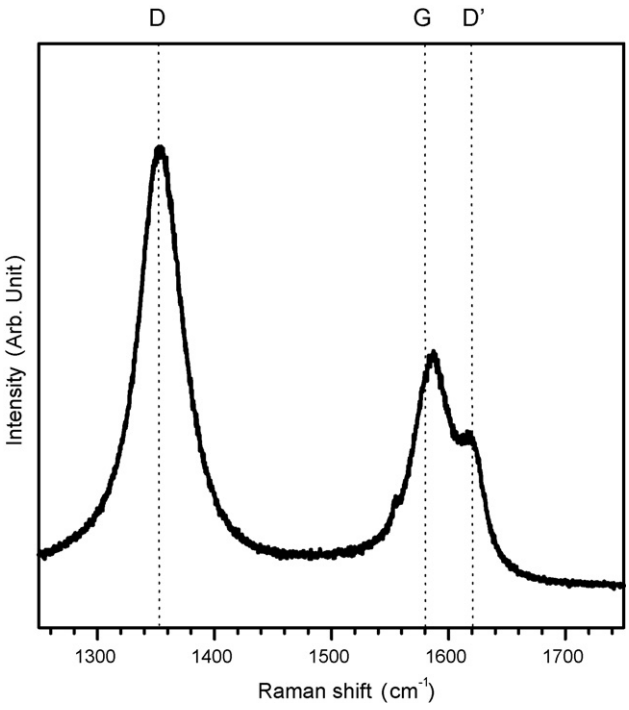

Fig. 2. Raman spectrum of carbon-coating on SUS304.

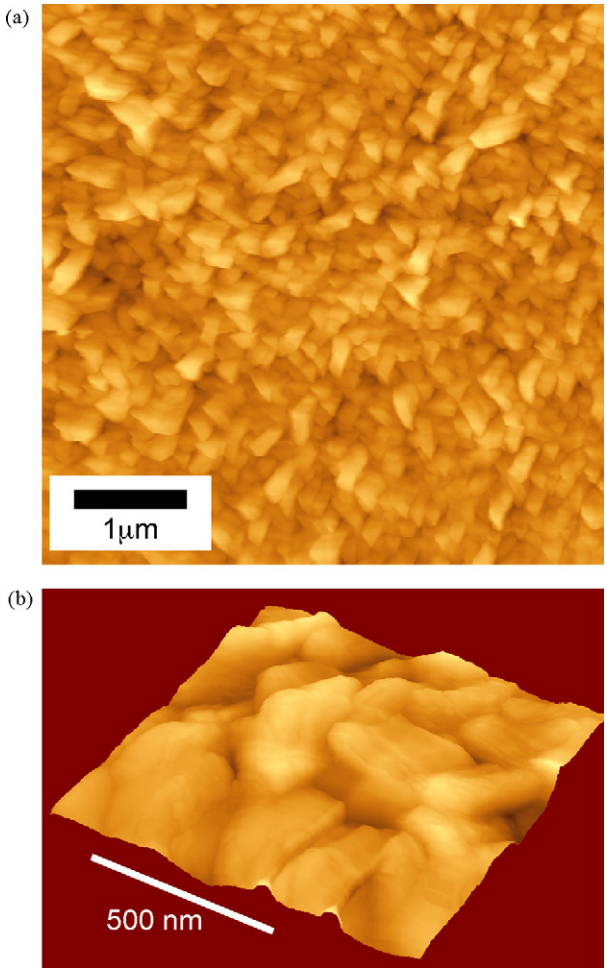

Fig. 3. AFM images (tapping mode) of carbon-coated SUS304. (a) 5-μm square image, and (b) 1-μm square 3D image.

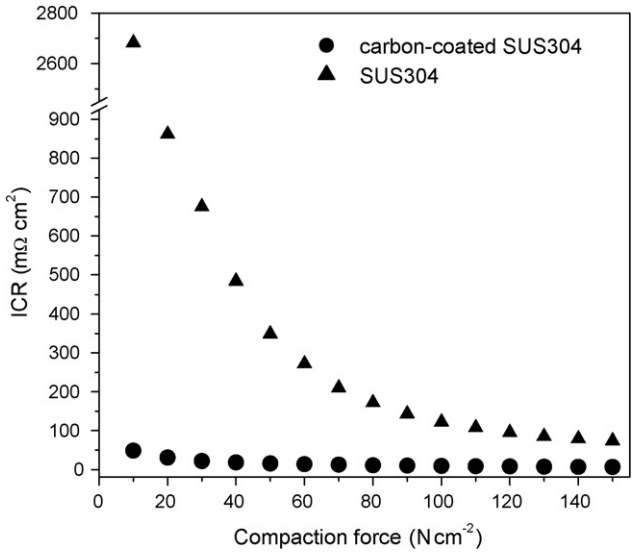

Fig. 4. Plots of interfacial contact resistances against compaction forces. Circles are ICRs for carbon-coated SUS304, and triangles are ICRs for SUS304.

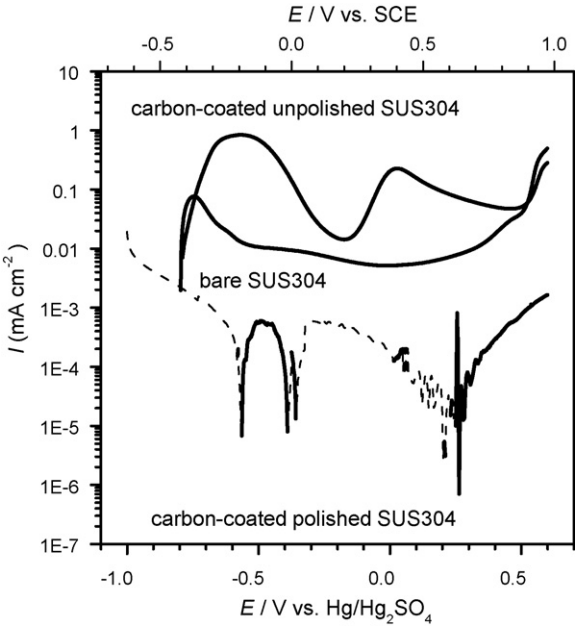

Fig. 5. Polarization curves of SUS304, carbon-coated polished SUS304, and carbon-coated unpolished SUS304 in a 0.5 mol dm^{-3} H_2SO_4 solution bubbled with N_2 at room temperature. Solid line and dashed line in the polarization curves shows anodic current and cathodic current, respectively.

AFM images, which one can see that the carbon-coating on SUS304 was dense. This morphology would be expected to prevent the electrolyte from penetrating into the carbon-coating.

3.2. Dynamic polarization behavior

Prior to the dynamic polarization measurement, a variation of the ICR against the compaction force was examined. The ICR values calculated in this study are the sum of $r_{\text{carbon paper/carbon-coated side of SUS304}}$ and $r_{\text{carbon paper/uncoated side of SUS304}}$, and they contain information about the uncoated side of SUS304. Hence, the ICR values for carbon-coated SUS304 should be higher than half of ICR for polished SUS304. However, the ICR values are lower than that value. This phenomenon might be due to the ultra-thin carbon-coating on the uncoated side by the incursion of plasma species into the space between the substrate and the ground electrode. In Fig. 4, the ICRs of carbon-coated SUS304 and SUS304 are plotted against the compaction force. Obviously, the ICRs of SUS304 were remarkably reduced by the surface carbon-coating. At a compaction force of 100 N cm^{-2}, the ICRs of SUS304 and carbon-coated SUS304 were about 122 mΩ cm^2 and 8.9 mΩ cm^2, respectively. Based on this result, it is considered that passive film was almost not formed in the carbon-coating process, and the carbon-coating acted as a high electric conductive layer on SUS304.

Fig. 5 shows the polarization curves of SUS304, carbon-coated polished SUS304, and carbon-coated unpolished SUS304 in a 0.5 mol dm^{-3} H_2SO_4 solution bubbled with N_2 at room temperature. Hereafter, solid lines and dashed lines in polarization curves show the anodic current and cathodic current, respectively. A large anodic current was observed for carbon-coated unpolished SUS304. On the other hand, the anodic current for carbon-coated polished SUS304 was much smaller than that for bare SUS304, leading to high corrosion resistance. This result is in good agreement with the result of AFM observation mentioned above. This different polarization behavior shows that the surface conditions before carbon-coating influence the corrosion resistances given by the carbon layer. This might be due to the passive film in the air. Polishing before carbon-coating can eliminate the major part of passive film on the surface of SUS304. Passive film formed in the air is mainly composed of chromium oxide. The surface chemical composition of unpolished SUS304 might become Cr-rich by re-precipitation of Cr due to the reduction of chromium oxide during the carbon-coating process, since good passive film is mainly composed of chromium oxide [22]. The effect of catalytic graphitization of Cr is lower than that of Fe or Ni [23]. Hence, the resulting carbon-coating was not sufficiently graphitized on the Cr-rich surface of SUS304. Based on the above result, since the carbon-coating on polished SUS304 imparted high corrosion resistance to SUS304, hereafter polished SUS304 is used as the substrate.

Next, dynamic polarization behavior under the PEFC cathode condition was examined. Fig. 6 shows the polarization curves of SUS304 and carbon-coated SUS304 in a 0.5 mol dm^{-3} H_2SO_4 solution bubbled with O_2 at 80 °C. In this measurement, HF was not added in order to clarify the corrosion behavior under the oxidizing atmosphere by O_2. The polarization curve for SUS304 showed a clear passive region in the range from −0.4 V to 0.4 V, since dissolved oxygen in the electrolyte solution helped the formation of passive film by the reaction with the metal ion. From 0.4 V, a large current was seen due to the metal dissolution through the passive film (transpassive region). For carbon-coated SUS304, anodic current was observed at around −0.5 V and over 0 V. These currents were quite small compared with that of SUS304. The desired current density related to metal dissolution in PEFC is reported to be less than 1 μA cm^{-2} (US

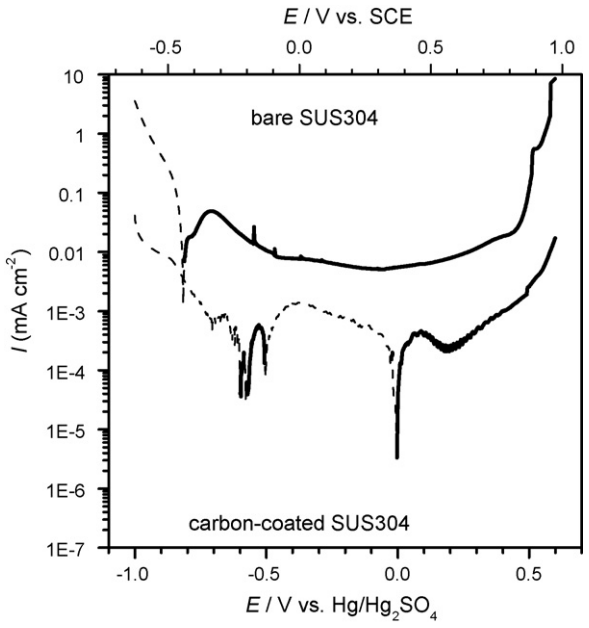

Fig. 6. Polarization curves of SUS304 and carbon-coated SUS304 in a 0.5 mol dm^{-3} H_2SO_4 solution bubbled with O_2 at 80 °C. Solid line and dashed line in the polarization curves show anodic current and cathodic current, respectively.

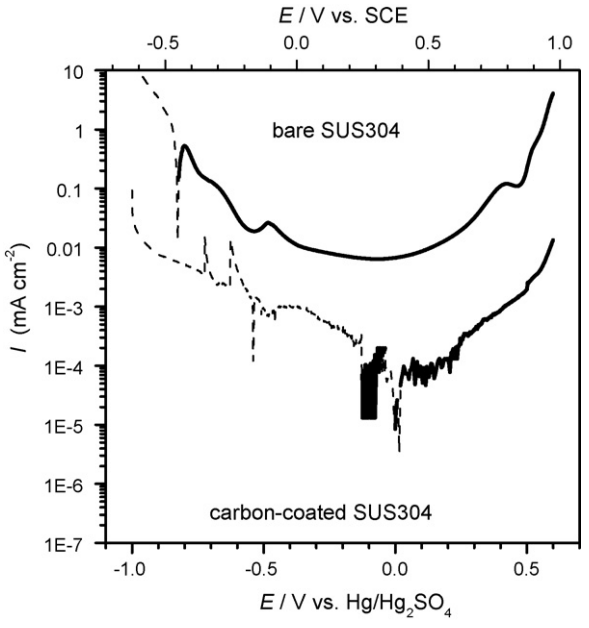

Fig. 7. Polarization curves of SUS304 and carbon-coated SUS304 in a 0.5 mol dm^{-3} H_2SO_4 solution bubbled with O_2 containing 2 ppm of HF at 80 °C. Solid line and dashed line in the polarization curves show anodic current and cathodic current, respectively.

DOE technical targets for bipolar plates with a corrosion rate of <1 μA cm^{-2} [24]). For carbon-coated SUS304, a value of current density less than 1 μA cm^{-2} is obtained below 0.4 V. Since the cathode potential under PEFC operation is reported to be about 0.226 V (=0.6 V vs. SCE), this carbon-coated SUS304 shows adequate corrosion resistance. In PEFC, the fluoride ion is released to the bipolar plates from a degraded proton exchange membrane (such as Nafion®). The influence of the fluoride ion on the dynamic polarization behavior of carbon-coated SUS304 is important. Then the dynamic polarization behavior in a 0.5 mol dm^{-3} H_2SO_4 solution bubbled with O_2 containing 2 ppm HF at 80 °C was examined. The results are shown in Fig. 7. The polarization curve for SUS304 in Fig. 7 is different from that in Fig. 6, that is, the passive region in Fig. 7 is narrower. This might be due to the fluoride ion in solution. The halogen ion generally causes pitting corrosion of SUS304 and the influence is in the order corresponding to $Cl^- > Br^- > I^- > F^-$ [25]. Since the concentration of F^- was quite low and the influence of F^- was not essentially so strong, typical pitting corrosion behavior (a rapid current increase) was not observed. On the other hand, there is almost no difference between the polarization curve for carbon-coated SUS304 in Fig. 7 and that in Fig. 6. This result shows that the corrosion resistance of carbon-coated SUS304 against F^- improved. The durability of Nafion® has been improving rapidly. Hence, the dissolution of the fluoride ion would drop to less than 2 ppm, which is the proposed experimental condition of PEFC [20]. Based on these discussions, it is considered that carbon-coated SUS304 is a candidate for bipolar plate material under the cathode condition.

The PEFC anode condition is an H_2 atmosphere. The influence of dissolved H_2 in an H_2SO_4 solution on the corrosion behavior would be weak. Hence, in this study, the dynamic polarization in an H_2SO_4 solution bubbled with H_2 containing no HF was not measured. Fig. 8 shows the polarization curves of SUS304 and carbon-coated SUS304 in a 0.5 mol dm^{-3} H_2SO_4 solution bubbled with H_2 containing 2 ppm of HF at 80 °C. The polarization behavior of SUS304 in Fig. 8 was similar to that in Fig. 7. This is due to the fluoride ion in the solution. Based on this result, the influence of the fluoride ion in an 80 °C H_2SO_4 solu-

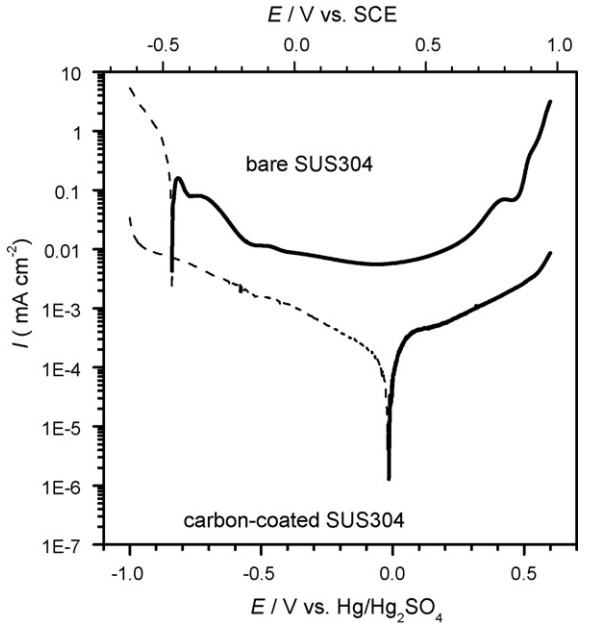

Fig. 8. Polarization curves of SUS304 and carbon-coated SUS304 in a 0.5 mol dm^{-3} H_2SO_4 solution bubbled with H_2 containing 2 ppm of HF at 80 °C. Solid line and dashed line in the polarization curves show anodic current and cathodic current, respectively.

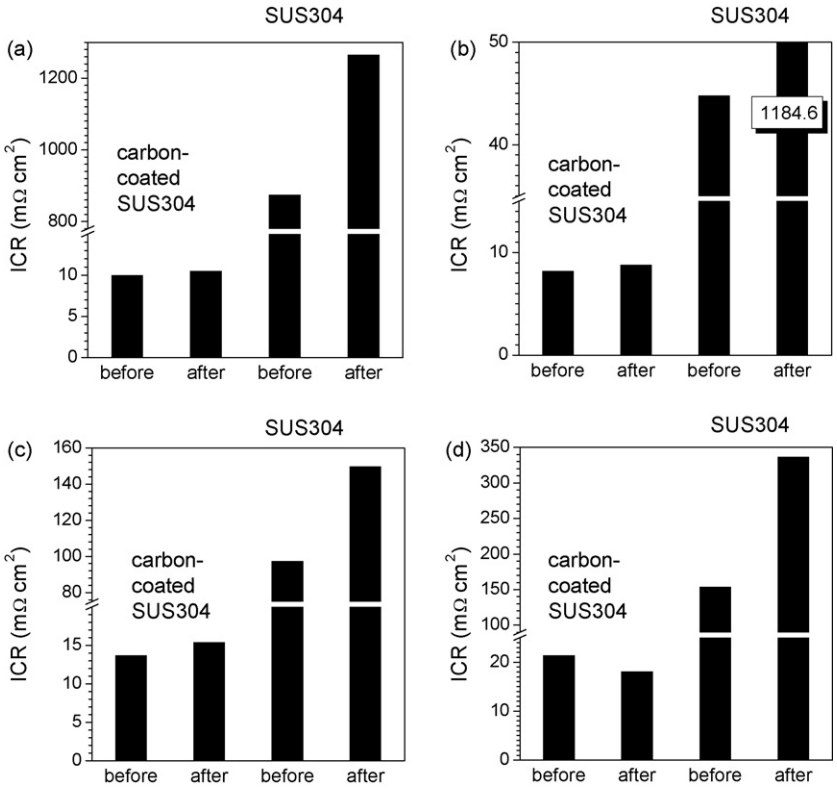

Fig. 9. Interfacial contact resistances for samples before and after dynamic polarization measurement. Polarization measurement conditions for (a)–(d) correspond to those of Figs. 5–8, respectively.

tion on the polarization behavior is more powerful than an O_2/H_2 atmosphere. Hence, the carbon-coating on SUS304 in this study was effective to improve the corrosion resistance in the solution containing the fluoride ion. Based on these polarization measurement results, carbon-coating is thought to be a candidate surface modification method giving high corrosion resistance to SUS304 as bipolar plate material under PEFC operating conditions.

3.3. Variation of ICRs after dynamic polarization measurement

Fig. 9 shows the variation of ICR values after the dynamic polarization measurement. Under all conditions, the ICR of SUS304 increased after the polarization measurement due to the growth of passive film. The difference in the ICRs of SUS304 before the polarization measurement is probably due to the different surface conditions from polishing. In particular, the oxidizing condition without the fluoride ion showed an extreme increase. This is due to the formation of high corrosion-resistant passive film. This result shows that SUS304 is not suitable as a current collector under PEFC operating conditions. On the other hand, the ICRs of carbon-coated SUS304 were almost unchanged after the polarization measurement. The difference in the ICRs of carbon-coated SUS304 before the polarization measurement and the decrease in the ICRs after the polarization measurement observed in (d) are probably due to the different surface conditions of the uncoated side of SUS304. This factor cannot be avoided at this stage. Based on this result, the ICRs of carbon-coated SUS304 were not affected by the polarization measurement under any condition, leading to the stable, high electric conductive layer on SUS304.

4. Conclusion

Carbon-coating on stainless steel (SUS304) was carried out by plasma-assisted CVD. Based on the result of a Raman measurement, the carbon-coating mainly consisted of sp^2-type carbon (conductive carbonaceous material). Carbon-coated SUS304 showed high electric conductivity compared with SUS304. This result showed the absence of passive film between the carbon-coating and SUS304. The dynamic polarization behavior of carbon-coated SUS304 under PEFC operating conditions improved in spite of the absence of passive film. The corrosion resistance of carbon-coated SUS304 depended on the polishing process of SUS304 but the reason was not clarified at this stage. It is concluded that the carbon-coating on SUS304 might be a candidate technique for the improvement of metal bipolar plates. Long-term potentiostatic experiments are under way to justify the use of carbon-coated SUS304.

Acknowledgement

The authors wish to thank Prof. Takeshi Abe (Kyoto University) for fruitful discussions.

References

[1] X. Li, I. Sabir, Int. J. Hydrogen Energy 30 (2005) 359.

[2] M. Arita, Fuel Cells 2 (2002) 10.
[3] T. Kinumoto, M. Inaba, Y. Nakayama, K. Ogata, R. Umebayashi, A. Tasaka, Y. Iriyama, T. Abe, Z. Ogumi, J. Power Sources 158 (2006) 1222.
[4] J. Wind, R. Späh, W. Kaiser, G. Böhm, J. Power Sources 105 (2002) 256.
[5] V. Mehta, J.S. Cooper, J. Power Sources 114 (2003) 32.
[6] T. Fukutsuka, T. Yamaguchi, Y. Matsuo, Y. Sugie, Z. Ogumi, Electrochemistry 75 (2007) 152.
[7] D.P. Davies, P.L. Adcock, M. Turpin, S.J. Rowen, J. Appl. Electrochem. 30 (2000) 101.
[8] H. Wang, M.A. Sweikart, J.A. Turner, J. Power Sources 115 (2003) 243.
[9] D.P. Davies, P.L. Adcock, M. Turpin, S.J. Rowen, J. Power Sources 86 (2003) 237.
[10] H. Wang, J.A. Turner, J. Power Sources 128 (2004) 193.
[11] H. Wang, M.P. Brady, K.L. More, H.M. Meyer III, J.A. Turner, J. Power Sources 138 (2004) 79.
[12] H. Wang, M.P. Brady, G. Teeter, J.A. Turner, J. Power Sources 138 (2004) 86.
[13] S. Joseph, J.C. McClure, R. Chianelli, P. Pich, P.J. Sebastian, Int. J. Hydrogen Energy 30 (2005) 1339.
[14] H. Wang, G. Teeter, J.A. Turner, J. Electrochem. Soc. 152 (2005) B99.
[15] R. Tian, J. Sun, L. Wang, Int. J. Hydrogen Energy 31 (2006) 1874.
[16] A.K. Iversen, Corros. Sci. 48 (2006) 1036.
[17] R. Tian, J. Sun, L. Wang, J. Power Sources 163 (2007) 719.
[18] T. Abe, T. Fukutsuka, M. Inaba, Z. Ogumi, Carbon 37 (1999) 1165.
[19] T. Fukutsuka, T. Abe, M. Inaba, Z. Ogumi, J. Electrochem. Soc. 148 (2001) A1260.
[20] R.L. Borup, N.E. Vanderborgh, Mater. Res. Soc. Symp. Proc. 393 (1995) 151.
[21] F. Tuinstra, J. Koenig, J. Chem. Phys. 53 (1970) 1126.
[22] I. Olefjord, H. Fischmeister, Corros. Sci. 15 (1975) 697.
[23] A. Oya, S. Otani, Carbon 17 (1979) 131.
[24] DOE Hydrogen Program FY 2006 Annual Progress Report, 2006, p. 822.
[25] M.A.C. de Castro, B.E. Wilde, Corros. Sci. 19 (1979) 923.